

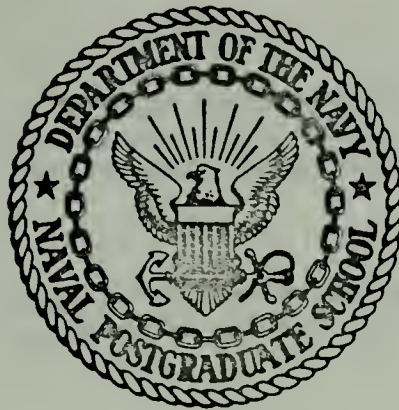
GLOBAL WEATHER PREDICTION MODEL  
DIFFERENCE SCHEMES

William Franklin Mihok

DUDLEY KNOX LIBRARY  
NAVAL POSTGRADUATE SCHOOL  
MONTEREY, CALIFORNIA 93940

# NAVAL POSTGRADUATE SCHOOL

## Monterey, California



# THESIS

GLOBAL WEATHER PREDICTION MODEL

DIFFERENCE SCHEMES

by

William Franklin Mihok

Thesis Advisor:

R. T. Williams

March 1974

T159609

*Approved for public release; distribution unlimited.*



Global Weather Prediction Model

Difference Schemes

by

William Franklin Mihok  
Lieutenant, United States Navy  
B.S., Pennsylvania State University, 1964

Submitted in partial fulfillment of the  
requirements for the degree of

MASTER OF SCIENCE IN METEOROLOGY

from the  
NAVAL POSTGRADUATE SCHOOL  
March 1974

Thesis  
M5814  
c.1

## ABSTRACT

One case of analytic data and one case of real data were numerically integrated using a 5-level baroclinic primitive equation global model of the general circulation. The feasibility of using a mixed second order and fourth order space differencing scheme to improve the phase speeds of meteorological waves was examined. The results indicate that mixed scheme tends to give a better representation of the phase speeds than the second order scheme does.





## TABLE OF CONTENTS

I.	INTRODUCTION - - - - -	11
II.	BAROCLINIC PRIMITIVE EQUATION MODEL- - - - -	12
	A. PRIMITIVE EQUATIONS- - - - -	12
	B. GRID - - - - -	15
	C. VERTICAL LAYERING- - - - -	15
	D. TIME DIFFERENCING- - - - -	18
	E. FOURTH ORDER MIXED SPACE DIFFERENCING- - - - -	19
III.	INITIAL CONDITIONS - - - - -	20
IV.	WAVE ANALYSIS METHOD - - - - -	23
V.	RESULTS- - - - -	24
VI.	CONCLUSIONS- - - - -	39
	APPENDIX A - - - - -	40
	APPENDIX B - - - - -	50
	LIST OF REFERENCES - - - - -	52
	INITIAL DISTRIBUTION LIST- - - - -	54
	FORM DD 1473 - - - - -	58



## LIST OF FIGURES

1. Location of Variables and Grid - - - - -	16
2. Vertical Layering- - - - -	17
3. Phase Angle vs Latitude for the Second Order Differencing - - - - -	25
4. Phase Angle vs Latitude for Mixed Scheme - - - - -	26
5. Interpolation for $\nabla\pi$ - - - - -	45



## LIST OF TABLES

I.	Average Movement of Analytic Wave per 24-Hours for a 72-Hour Forecast for both Differencing and the Mixed Scheme - - - - -	27
II.	Initial Positions of High Centers and Forecast Positions of the Second Order Scheme and the Mixed Scheme - - - - -	38
III.	Initial Positions of Low Centers and Forecast Positions of the Second Order Scheme and the Mixed Scheme - - - - -	38



## LIST OF CHARTS

A.	Initial Surface Pressure Field - - - - -	29
B.	12-Hour Forecast, Second Order Scheme- - - - -	30
C.	24-Hour Forecast, Second Order Scheme- - - - -	31
D.	36-Hour Forecast, Second Order Scheme- - - - -	32
E.	48-Hour Forecast, Second Order Scheme- - - - -	33
F.	12-Hour Forecast, Mixed Scheme - - - - -	34
G.	24-Hour Forecast, Mixed Scheme - - - - -	35
H.	36-Hour Forecast, Mixed Scheme - - - - -	36
I.	48-Hour Forecast, Mixed Scheme - - - - -	37





## LIST OF SYMBOLS AND ABBREVIATIONS

$A$	- Arbitrary constant in the stream function
$A_m$	- Arbitrary constant for the Fourier series cosine terms
$a$	- Earth's radius
$B$	- Arbitrary constant in the stream function
$B_m$	- Arbitrary constants for the Fourier series sine terms
CDC	- Control Data Corporation
$C_m$	- Arbitrary constants for the Fourier series combined terms
$c_p$	- Specific heat for dry air at constant pressure
$c$	- Wave speed
$D$	- Lateral diffusion for the quantity indicated by the subscript
$D_T$	- Lateral diffusion of heat
$D_q$	- Lateral diffusion of specific humidity
$D_m$	- Lateral diffusion of momentum
FNWC	- Fleet Numerical Weather Central
$F$	- Frictional stress
$f$	- Coriolis parameter
$\bar{f}$	- Coriolis parameter at 45° north
$g$	- Acceleration of gravity
$H$	- Diabatic heating
$i$	- Grid index in the x-direction (east-west)
$j$	- Grid index in the y-direction (north-south)
$M$	- Stands for $\phi$ , $T$ , $q$ , and $w$
$m$	- Wave number



mb	- Millibars
NPS	- Naval Postgraduate School
NACA	- National Advisory Committee on Aeronautics
N	- Wave number plus one - $m + 1$
n	- Degree of the Legendre function
P	- Pressure
$P_n^m$	- Legendre function of order m and degree n
Q	- Moisture source/sink term
q	- Specific humidity
R	- Specific gas constant for dry air
t	- Time
T	- Temperature
u	- Zonal wind
$\vec{V}$	- Horizontal vector velocity - (u,v)
v	- Meridional wind
W	- Stands for u or v
w	- Measure of vertical velocity, positive upward $w = -\dot{\sigma} = -\frac{d\sigma}{dt}$
$\Delta t$	- Time increment
$\Delta x$	- Distance increment in the x-direction - $a \Delta \lambda \cos \theta$
$\alpha$	- Specific volume
$\delta_m$	- Phase angle for wave number m
$\theta$	- Latitude, positive northward from south pole
$\Delta \theta$	- Distance increment in the latitudinal direction
$\lambda$	- Longitude, positive eastward from Greenwich
$\Delta \lambda$	- Distance increment in longitudinal direction
$\nu$	- Angular wave velocity



$\pi$	- Terrain pressure parameter
$\sigma$	- Dimensionless vertical coordinate $0 \leq \sigma \leq 1$ , increasing downward
$\dot{\sigma}$	- Measure of vertical velocity - $\frac{d\sigma}{dt}$ , $-w$
$\Phi$	- Geopotential
$\psi$	- Stream function
$\nabla$	- Del operator (horizontal)
$\nabla^2$	- Laplacian operator (horizontal)



## ACKNOWLEDGEMENTS

The author wishes to express his thanks to Dr. R. T. Williams for his patient guidance without which this project would never have been completed, Lt. W. T. Elias, USN, for the original Fortran deck of the model and for his assistance throughout the project, the staff of the W. R. Church Computer Center of the Naval Postgraduate School for providing the many hours of computer time required to complete this project and finally to my wife who put up with many lonely nights during the past year.





## I. INTRODUCTION

A baroclinic primitive equation model using a global, staggered, spherical, sigma coordinate system which was originally written by Dr. F. J. Winninghoff and which is now being developed by the United States Navy Fleet Numerical Weather Central (Elias, 1973) was used in this study. The purpose of this investigation was to modify the horizontal space difference equations to a mixed second and fourth order scheme with the aim of improving the phase speeds of the meteorological waves, as proposed by Williams (1972). Real time data (Elias, 1973) and analytic data using an analytic spherical harmonic stream function (Neatam, 1946) were used as initial conditions. The use of the analytic case allowed the control of temperature and moisture distributions, predominant wave number, phase speed and wave amplitude.



## II. BAROCLINIC PRIMITIVE EQUATION MODEL

The governing differential equations, written in vector form, are similar to sets used by Smagorinsky et al (1965), Arakawa, et al (1969) and Kesel and Winninghoff (1972). The integrations were carried out on a global, spherical, staggered, sigma coordinate system using the conservative-type difference equations based on the procedure of Arakawa (1966). The complete set of finite difference equations are given in Kesel and Winninghoff (1972) for the non-staggered, polar stereographic grid. Appendix A contains the finite difference equations for the spherical, sigma, staggered system of equations. The heating, moisture, friction and diffusion finite difference terms are given in Kesel and Winninghoff (1972).

### A. PRIMITIVE EQUATIONS

The following are the equations for the model in spherical, sigma ( $\sigma$ ) coordinates.

The dimensionless vertical coordinate is:

$$\sigma = P/\pi .$$

The vertical velocity measure is defined as:

$$w = - \frac{d\sigma}{dt} = - \dot{\sigma} .$$

The latitudinal component of the equation of motion is:

$$\frac{\partial u\pi}{\partial t} = - \frac{1}{a \cos \theta} \left[ \frac{\partial (uu\pi)}{\partial \lambda} + \frac{\partial (uv\pi \cos \theta)}{\partial \theta} \right]$$



$$\begin{aligned}
& + \frac{\pi \partial(wu)}{\partial \sigma} + \frac{\pi uv \tan \theta}{a} + \pi v f \\
& - \frac{1}{a \cos \theta} \left[ \pi \frac{\partial \phi}{\partial \lambda} + \frac{RT}{\partial \lambda} \frac{\partial \pi}{\partial \lambda} \right] + \pi F_2 + D_u .
\end{aligned} \tag{1}$$

The longitudinal-component of the equation of motion is:

$$\begin{aligned}
\frac{\partial v \pi}{\partial t} &= \frac{1}{a \cos \theta} \left[ \frac{\partial (uv \pi)}{\partial \lambda} + \frac{\partial (vv \pi \cos \theta)}{\partial \theta} \right] \\
& + \frac{\pi \partial(wv)}{\partial \sigma} + \frac{\pi uu \tan \theta}{a} - \pi u f \\
& - \frac{1}{a} \left[ \pi \frac{\partial \phi}{\partial \theta} + \frac{RT}{\partial \theta} \frac{\partial \pi}{\partial \theta} \right] + \pi F_y + D_v .
\end{aligned} \tag{2}$$

The First Law is:

$$\begin{aligned}
\frac{\partial \pi T}{\partial t} &= - \frac{1}{a \cos \theta} \left[ \frac{\partial (\pi u T)}{\partial \lambda} + \frac{\partial (\pi v T \cos \theta)}{\partial \theta} \right] \\
& + \frac{\pi \partial(wT)}{\partial \sigma} \\
& + \frac{RT}{c_p \sigma} \left[ -w \pi + \sigma \left( \frac{\partial \pi}{\partial t} + \frac{1}{a \cos \theta} \left[ u \frac{\partial \pi}{\partial \lambda} + v \frac{\partial \pi}{\partial \theta} \cos \theta \right] \right) \right] \\
& + \pi H + D_T .
\end{aligned} \tag{3}$$

The Moisture Equation is:

$$\begin{aligned}
\frac{\partial q \pi}{\partial t} &= - \frac{1}{a \cos \theta} \left[ \frac{\partial (\pi u q)}{\partial \lambda} + \frac{\partial (\pi v q \cos \theta)}{\partial \theta} \right] \\
& + \pi \frac{\partial(wq)}{\partial \sigma} + Q \pi + D_q .
\end{aligned} \tag{4}$$



The continuity equation is:

$$\frac{\partial \pi}{\partial t} = - \frac{1}{a \cos \theta} \left[ \frac{\partial (u\pi)}{\partial \lambda} + \frac{\partial (v\pi \cos \theta)}{\partial \theta} \right] + \pi \frac{\partial w}{\partial \sigma} . \quad (5)$$

The Hydrostatic Equation is:

$$\frac{\partial \phi}{\partial \sigma} = - \frac{RT}{\sigma} \quad (6)$$

In the above equations,  $u$  is the zonal wind component;  $v$ , the meridional wind component;  $\pi$ , the terrain pressure,  $T$ , the temperature;  $f$ , the Coriolis parameter;  $\phi$ , the geopotential;  $q$ , the specific humidity;  $H$ , the diabatic heating;  $F$ , the frictional stress;  $D$ , the lateral diffusion of momentum;  $D_T$ , the lateral diffusion of heat;  $D_q$ , the lateral diffusion of moisture source/sink term;  $P$ , the pressure;  $a$ , the radius of the earth;  $\lambda$ , longitude and  $\theta$ , the latitude.

Kesel and Winninghoff (1972) modified the pressure gradient terms as suggested by Kurihara (1968) to reduce the inconsistent truncation error which arises as a result of the sensitivity of the model to variations in the height and character of the terrain. The value of the geopotential is interpolated at neighboring gridpoint locations to the same pressure surface as at the computation point to enable one to compute to geopotential gradients on pressure surfaces which are thus synthesized locally around each computational point. The pressure gradient term in sigma coordinates is:

$$- \nabla_p \phi = - \nabla_\sigma \phi \frac{RT}{\pi} \nabla \pi . \quad (7)$$





Solving for the gradient of  $\pi$  in component form one gets,

$$\frac{\partial \pi}{\partial \lambda} = \frac{\pi}{RT} \left[ \frac{\partial \Phi}{\partial \lambda}_p - \frac{\partial \Phi}{\partial \lambda}_\sigma \right] \quad (8)$$

$$\frac{\partial \pi}{\partial \theta} = \frac{\pi}{RT} \left[ \frac{\partial \Phi}{\partial \theta}_p - \frac{\partial \Phi}{\partial \theta}_\sigma \right] \quad (9)$$

It is shown in Appendix A that the right hand side of equations (8) and (9) are the sum of the thicknesses between the sigma surface and the pressure surface to the right and left of the computational points. Since the thickness depends only upon the mean temperature of the layer in question, the thickness equation is used to solve equations (8) and (9). The mean temperature is obtained by interpolation as indicated in Appendix A.

## B. GRID

The longitudinal and latitudinal grid increments were ten degrees for the mass and velocity fields. The geopotential ( $\Phi$ ), temperature ( $T$ ), specific humidity ( $q$ ), and the vertical-velocity ( $w = -\dot{\sigma}$ ) were carried at the poles. When  $\Phi$ ,  $T$ ,  $q$ ,  $w$  and  $\pi$  were needed at a velocity point they were taken as the average of the four surrounding mass points. Figure 1 represents the staggered grid and location of the variables.

## C. VERTICAL LAYERING

Figure 2 is the vertical layering as described by Elias (1973). The basic variables, as indicated, are carried at the center of each layer except that the specific humidity ( $q$ ) is carried at the lower three layers only. The vertical velocity ( $w$ ) is carried at the interface



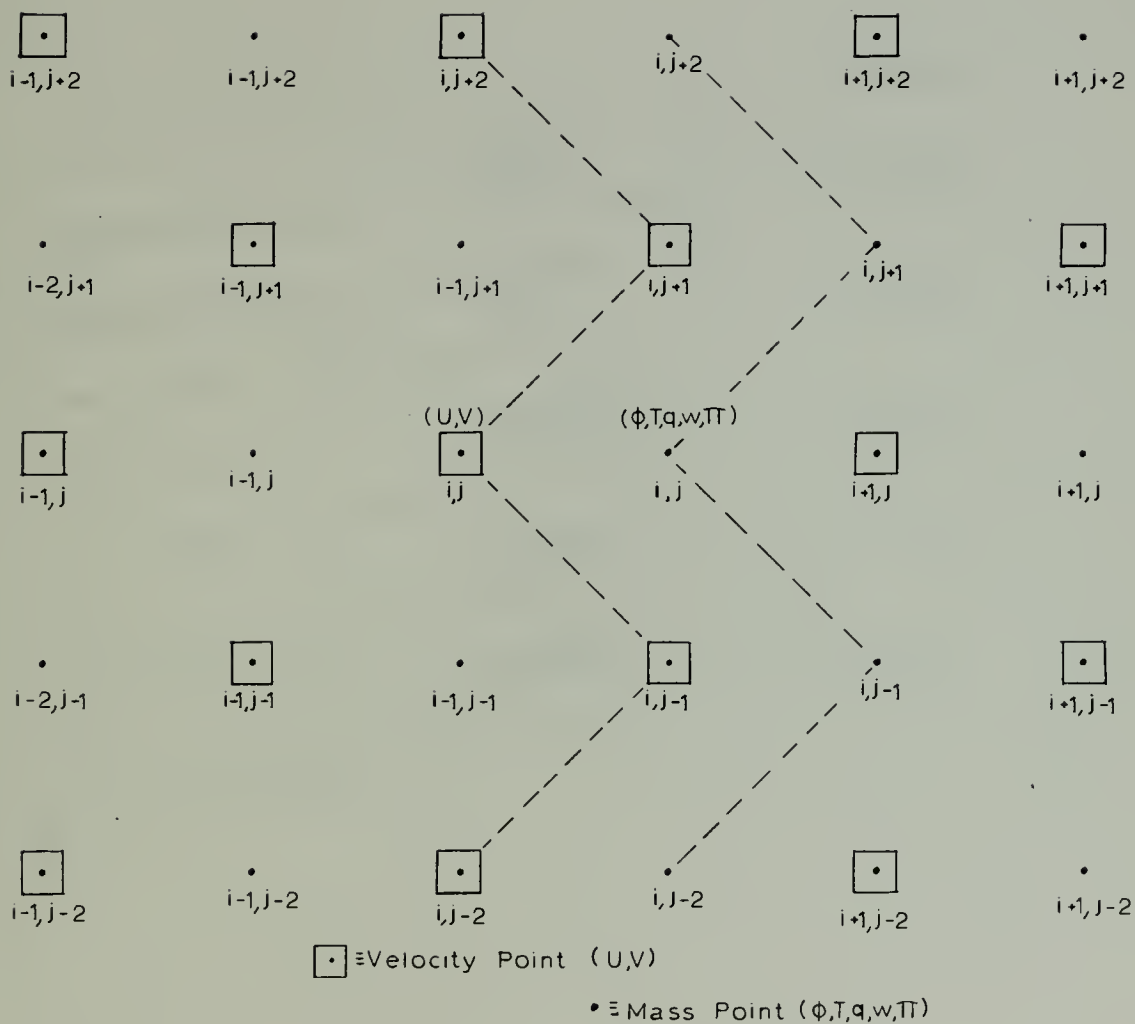


Figure 1. Location of Variables and Grid.



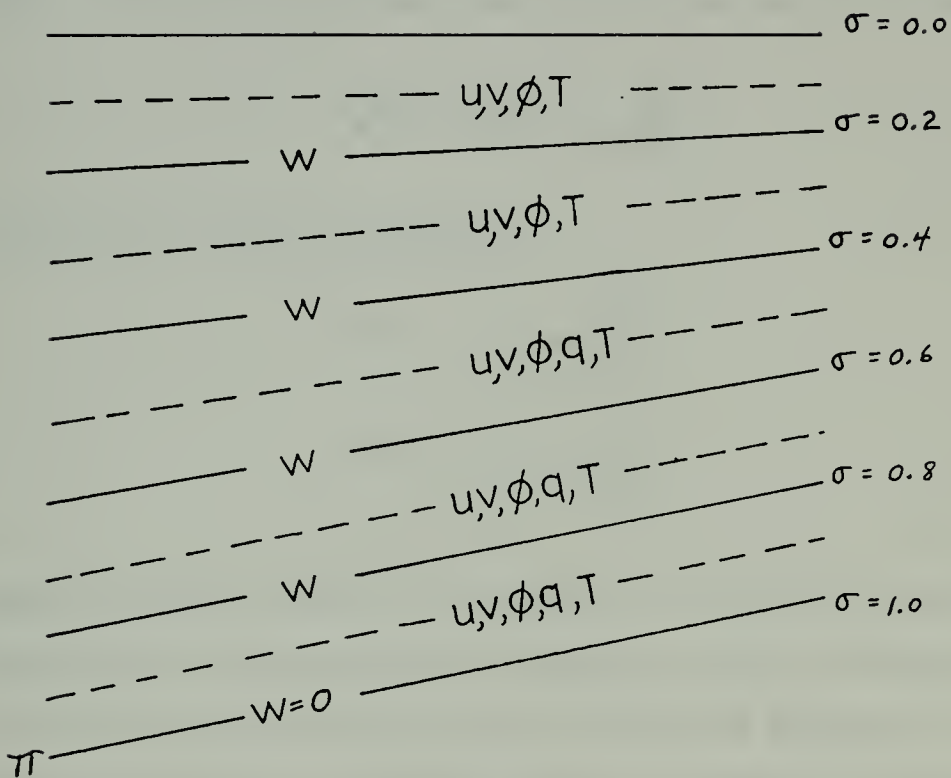


Figure 2. Vertical Layering



between layers. The vertical coordinate, sigma ( $\sigma$ ) was defined by Phillips (1957).

#### D. TIME DIFFERENCING

The two finite difference techniques that were used were the centered difference scheme and the Matsuno (Euler-backward) difference scheme. The finite difference equation for the centered technique is

$$F^{t+1} = F^{t-1} + 2\Delta t \frac{\partial F^t}{\partial t}$$

and that for the Matsuno scheme is

$$F^k = F^t + \Delta t \frac{\partial F^t}{\partial t}$$

$$F^{t+1} = F^t + \Delta t \frac{\partial F^t}{\partial t} .$$

Since the centered scheme is not feasible for the first time step and also produces a computational mode (Haltiner, 1971), the Matsuno scheme was used for the initial time step of each 3-hour integration to reduce solution separation. The Matsuno scheme also selectively dampens high frequency waves (Haltiner, 1971). The Arakawa technique (Langlois and Kwok, 1969) of averaging quantities involved in the longitudinal derivatives is used. This allowed a time step of ten minutes to be used. Without this technique, the Von Neuman linear computational stability criterion (Haltiner, 1971) would require a two and one half minute time step because of the longitudinal grid distance at 85° latitude which is only 47 kilometers.





The lateral diffusion, friction, convective condensation and large scale condensation are computed at every time step while heating is computed every six time steps (Kesel and Winninghoff, 1972).

#### E. FOURTH ORDER MIXED SPACE DIFFERENCING

Williams (1972) found that the stability criterion for fourth order unstaggered space differencing required a time step which was 27% smaller than that for second order space differencing. He then noted that the phase speed of the meteorological wave is independent of the difference approximation which is used for the pressure force term. A mixture of fourth order differencing in the advection terms and the divergence term in the continuity equation and second order differencing in the pressure force term was proposed. The stability criterion for this mixed scheme was found to require a time step that was only 14% smaller than that of the second order scheme. Thus the mixed differencing allows a larger time step while giving fourth order accuracy in the phase speed of the meteorological wave. Appendix B presents the fourth order differencing of the advection terms and the divergence term of the continuity equation. A time step of 8 minutes was used for this scheme.



### III. INITIAL CONDITIONS

Two cases, one using real data and the other analytic data, were used for initialization of both the second order and mixed differencing schemes. The real data was produced external to the main program on a Northern Hemispheric FNWC 63 x 63 grid. The analytic data with known phase propagation was produced following the work of Neamton (1946), Gates (1962), Heburn (1972) and Elias (1973). The real data were fields analyzed by FNWC objective schemes.

The main program was used to interpolate the data so that values at 5° latitude-longitude intersections were available on the Northern Hemisphere (Elias, 1973). The data was then reflected into the Southern Hemisphere. In both cases, the input data consisted of temperature analyses for the Northern Hemisphere at 12 constant pressure levels from 1000 to 50 mb, height analyses at ten of these levels, moisture analyses at four levels from the surface to 500 mb, sea level pressure and sea surface temperature. Monthly mean surface temperature fields were used to derive an albedo field (Dickson and Posey, 1967). In both cases the terrain height was set to zero. For the barotropic analytic case heating, convective adjustment and friction were turned off.

If one assumes nondivergent horizontal flow, harmonic wave solutions of the complete vorticity equation can be obtained for the sphere (Neamton, 1946). These solutions give the velocity of propagation of the wave. The solution of the  $\psi$  field (Elias, 1973) was found to be

$$\psi = A \sin (m\lambda - vt) P_n^m (\sin \theta) - B a^2 \sin \theta + C P_n (\sin \theta) \quad (1)$$



where A, B and C are constants to be determined, a is the radius of the earth, m is the hemispheric wave number,  $v/m$  is the angular phase speed of the wave (radians/second),  $P_n$  denotes the Legendre polynomial and  $P_n^m$  represents the associated Legendre function.

If  $C = 0$  and  $n = m + 1$  (Elias, 1973), equation (1) reduces to

$$\psi = A \sin (m\lambda - vt) (2N!/2^N N!) \sin \theta (\cos \theta)^6 - B a^2 \sin \theta \quad (2)$$

The constant A is arbitrary and proportional to the wave amplitude. It was shown by Haurwitz (1946) that the solution obtained for  $\psi$  implies the existence of a velocity distribution over a sphere such that the angular velocity of the westerly current is made up of the sum of three terms. The first, B, is constant over the sphere; the second term varies along a meridian but is constant around a latitude circle; and the third term represents the angular phase speed which is given by

$$v/m = B \frac{n(n+1)-2}{n(n+1)} - \frac{2\Omega}{n(n+1)} \quad (3)$$

where  $\Omega$  is the earth's rotation. For the analytic experiment A was chosen as  $1000 \text{ m}^2 \text{ sec}^{-1}$ , m as 6, n as 7 and B as  $8 \times 10^{-7} \text{ sec}^{-1}$ . The solution of equation (3) gives an angular velocity of  $-9^\circ$  longitude/day (toward the west). Since wave number six was used, integrations were performed for only one-sixth of a latitude circle with the remaining five-sixths being set equal to the first part. This resulted in a 40% saving of computer time for the analytic case only.

The geopotential fields were derived by solution of the linear balance equation and the temperatures, constant at each pressure surface,



were consistent with the National Advisory Committee for Aeronautics (NACA). Both the geopotential and temperature fields were derived as shown by Elias (1973).

The wind field was produced following the work of Elias (1973) by using the finite difference expressions

$$u = - \frac{1}{a} \frac{\Delta\psi}{\Delta\theta} \quad (4)$$

$$v = \frac{1}{a \cos \theta} \frac{\Delta\psi}{\Delta\lambda} \quad (5)$$

where  $a$  is the earth's radius,  $\Delta\theta$  is the latitudinal distance increment and  $\Delta\lambda$  is the longitudinal distance increment. Poleward of  $25^\circ$  latitude the initial geopotential field,  $\phi_o$ , was retained and the  $\psi$ -field was obtained by the solution of the linear balance equation,

$$\nabla^2 \psi + \nabla\psi \cdot \nabla f/f = \nabla^2 \phi_o/f \quad (6)$$

Equatorward of  $25^\circ$  latitude the  $\psi$ -field was determined using,

$$\psi = \phi_o/\bar{f}$$

where  $\bar{f}$  is a mean Coriolis parameter. A new geopotential field ( $\phi$ ) was obtained using

$$\nabla^2 \phi = (f\nabla^2 \psi + \nabla\psi \cdot \nabla f) .$$

At  $25^\circ$  latitude,  $\psi$  and  $\phi$ , were a combination of half the value of the poleward case and half of the equatorward case.





#### IV. WAVE ANALYSIS METHOD

A Fourier series was determined at each five degrees of latitude around the latitude circle. With this technique, the phase angles and amplitudes of each wave number around a latitude circle can be calculated. A Fourier series can be expressed as follows (Heburn, 1972):

$$\begin{aligned} F(x) &= A_o + \sum_m (A_m \cos mx + B_m \sin mx) \\ &= C_o + \sum_m (C_m \cos (mx - \delta_m)) \end{aligned}$$

where 
$$C_m = \frac{B_m}{\sin(\delta_m)} = \frac{A_m}{\cos(\delta_m)}$$

and

$$\delta_m = \tan^{-1} (B_m/A_m) .$$

The analytic experiment involved an input stream function of wave number six. The values of primary interest were  $\delta_6$  and  $C_6$  which are the phase angle and amplitude of wave number six. Other angles and amplitudes were extracted, especially in the real data case.



## V. RESULTS

Two experiments will be presented in this section. The first experiment was performed with analytic fields and the second with FNWC analyzed fields from 1200Z 10 May 1973.

As indicated in section III the angular phase speed for wave number six was  $-9^\circ$  longitude/day (toward the west). A 72-hour forecast of surface pressure was made by both the second and mixed order differencing. The changes in phase angle vs latitude were plotted for both cases and are shown in Figures 3 and 4. Table I summarizes the average angular movement per 24-hour the entire 72-hour forecast for both differencing schemes. It should be noted that the mixed differencing scheme propagated the wave slower to the west than the second order scheme. The barotropic Rossby equation (Holton, 1972) is given as

$$C = \bar{u} - \frac{\beta}{(k^2 + m^2)}$$

where  $\beta$  is  $\frac{df}{dy}$ ,  $f$  is the Coriolis parameter,  $\bar{u}$  is the mean zonal flow,  $k$  is the zonal wave length,  $m$  is the wave number and  $C$  is the zonal phase speed. Since the quantities  $\beta$ ,  $k$  and  $m$  are constant the phase speed,  $C$ , depends only upon the mean zonal flow. Fourth-order differencing should give a better approximation for the effect of the mean zonal wind,  $\bar{u}$ , and therefore the westward movement of the wave would be slower than that of the second order differencing case. It would appear that the mixed differencing scheme does give a better solution.



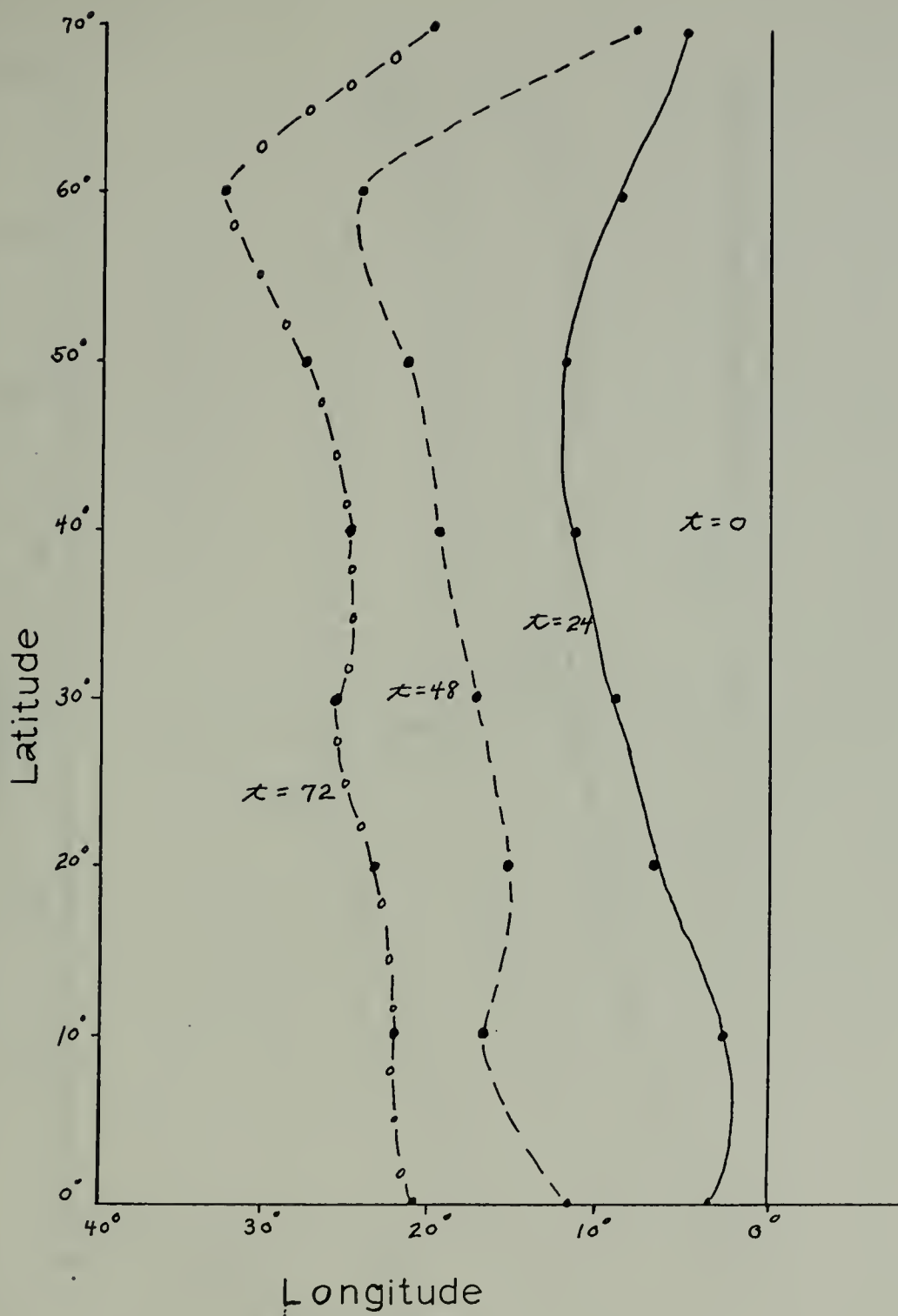


Figure 3. Phase Angle vs Latitude for the Second Order Scheme.



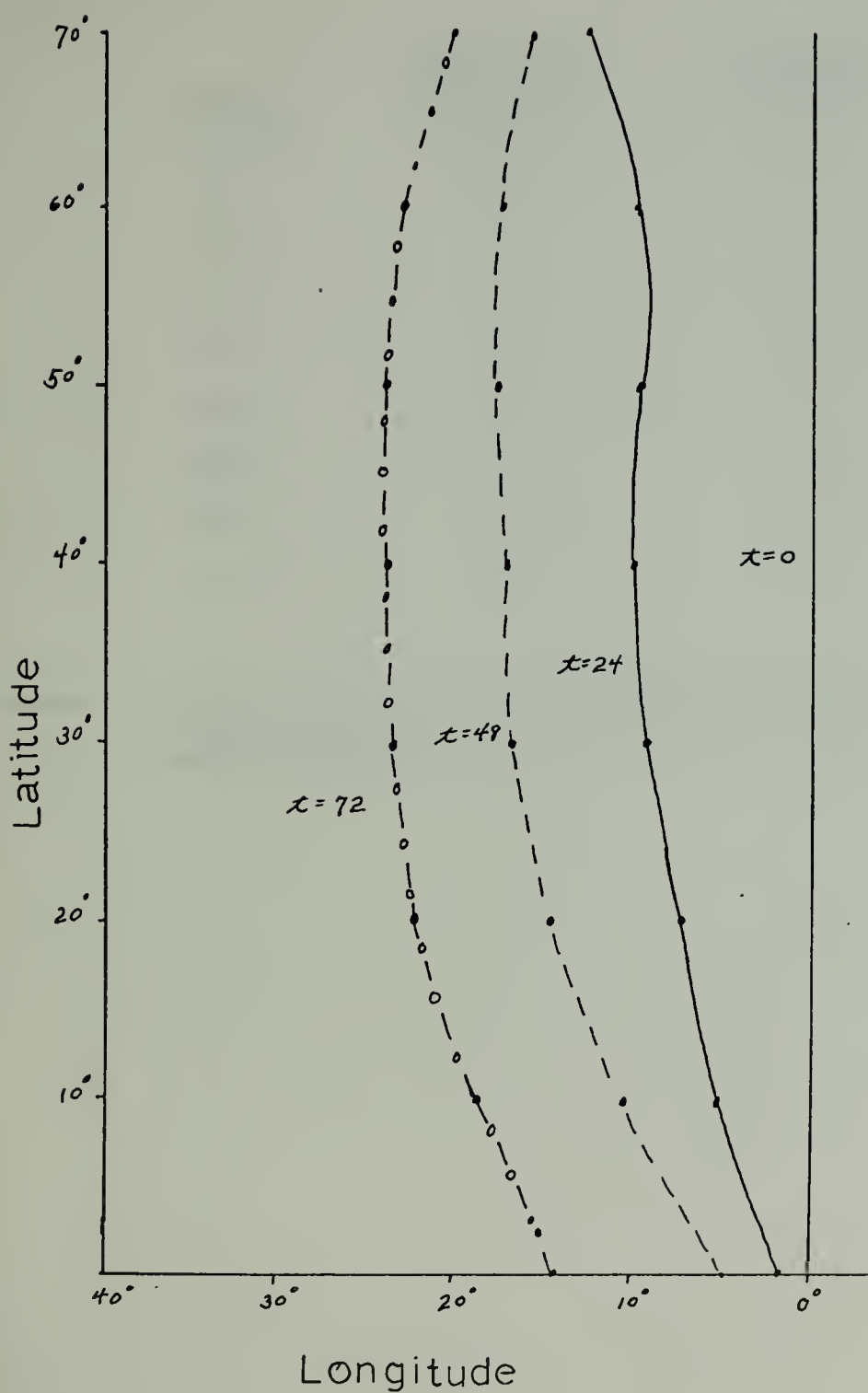


Figure 4. Phase Angle vs Latitude for the Mixed Scheme.





LATITUDE	SECOND ORDER DEG LAT/DAY	MIXED SCHEME DEG LAT/DAY
70°	-12.6°	-4.8
60°	-10.3°	-7.9
50°	-9.2°	-7.4
40°	-8.5°	-7.5
30°	-7.7°	-7.2
20°	-7.3°	-7.6
10°	-7.0°	-6.5
0°	-4.6°	-3.6

TABLE I. Average Movement of Analytic Wave per 24-Hours for a 72-Hour Forecast for Both Second Order Differencing and the Mixed Scheme.



A 48-hour forecast was also made by both the second order and mixed differencing schemes using analyzed FNWC data fields. Chart A is the initial analyzed surface pressure field, Charts B through E are the 12-, 24-, 36- and 48-hour forecasts produced by the second order scheme and Charts F through I are the corresponding forecasts produced by the mixed differencing scheme. Table II lists five high pressure centers and Table III lists seven low pressure centers with their initial position and both the 48-hour second order and 48-hour mixed scheme forecast positions. As can be seen each high pressure center was forecast at least five degrees farther to the east by the mixed differencing scheme. Low pressure centers 1 and 3 also were forecast five degrees farther to the east by the mixed scheme while low centers 2 and 4 were moved very little by both differencing schemes. Low number 5 was the only low that was moved slower than the second order scheme. Low number 6 was developed into two centers by both forecast schemes. Only the forecast position of the major center was listed in Table III. The mixed scheme moved this center nine degrees farther than the second order scheme. Center number 7 was also initially a single center but was developed into three small centers with the second order forecast scheme. The mixed scheme maintained the more realistic single center system near its initial position.





Chart A. Initial Surface Pressure Field.



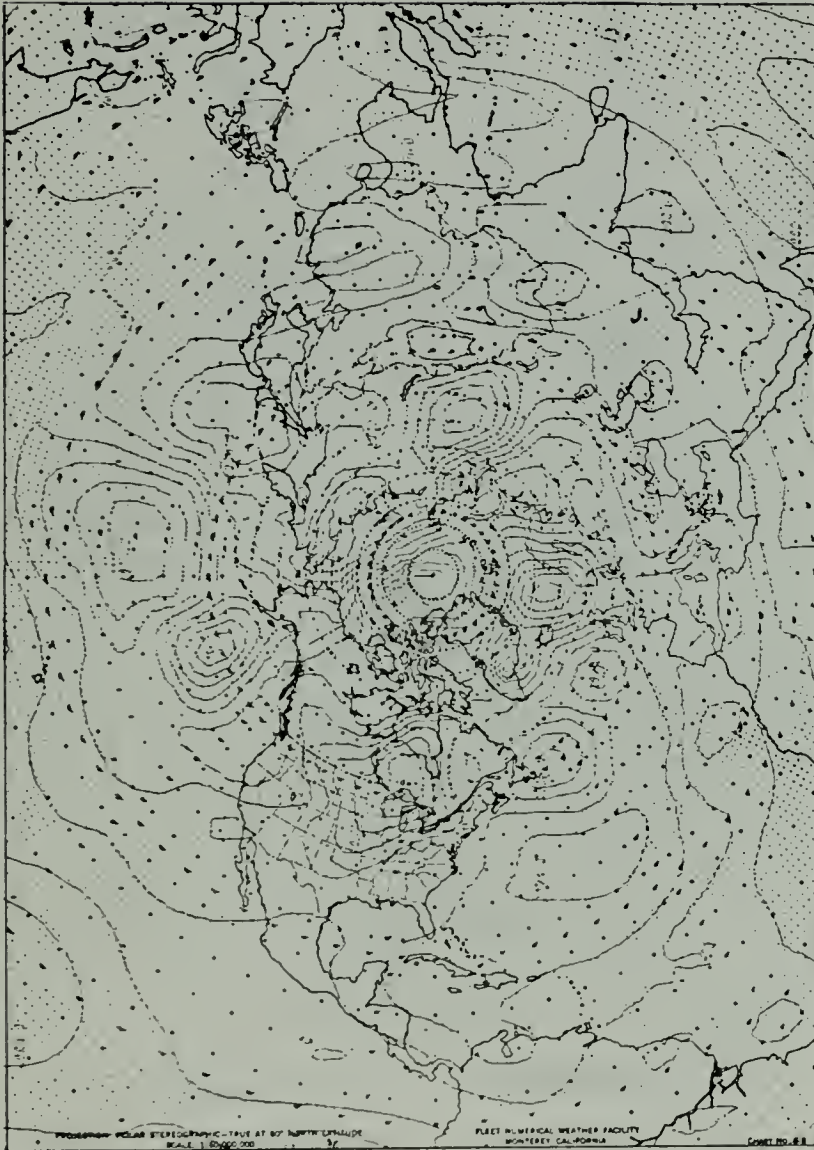


Chart B. 12-Hour Forecast, Second Order Scheme.





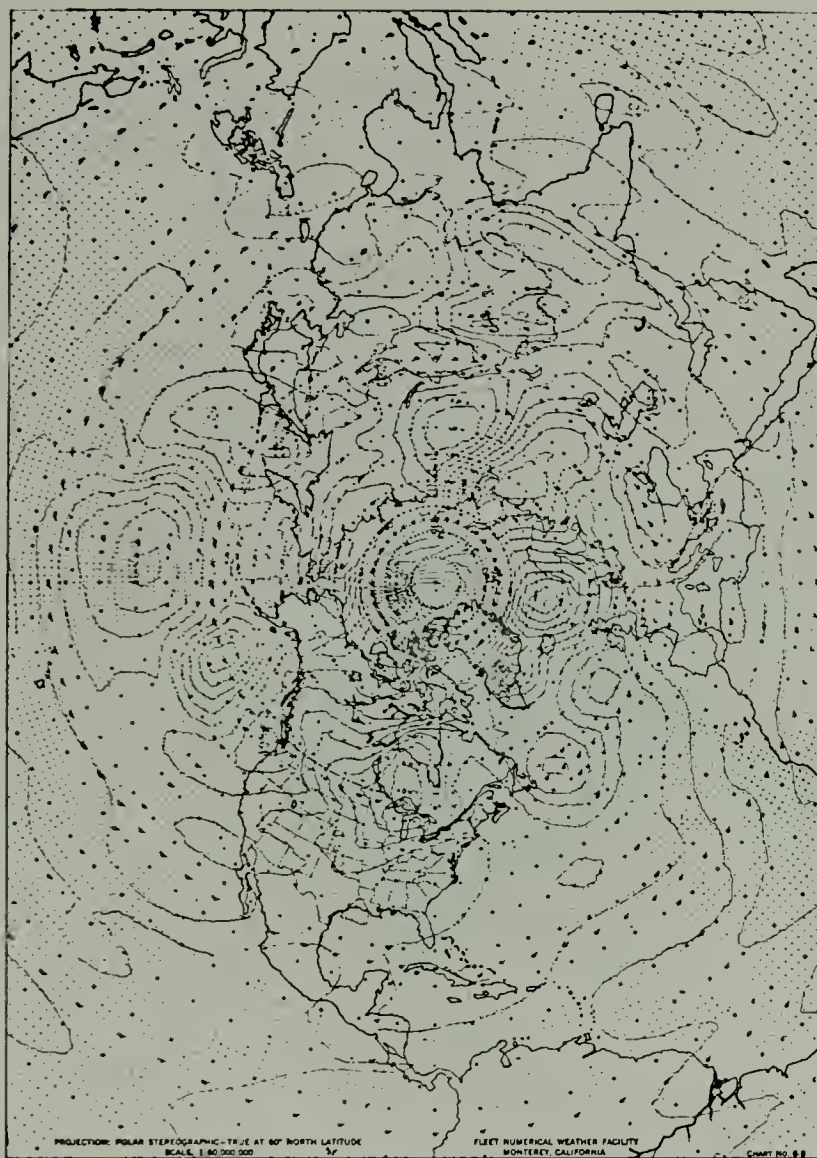


Chart C. 24-Hour Forecast, Second Order Scheme.



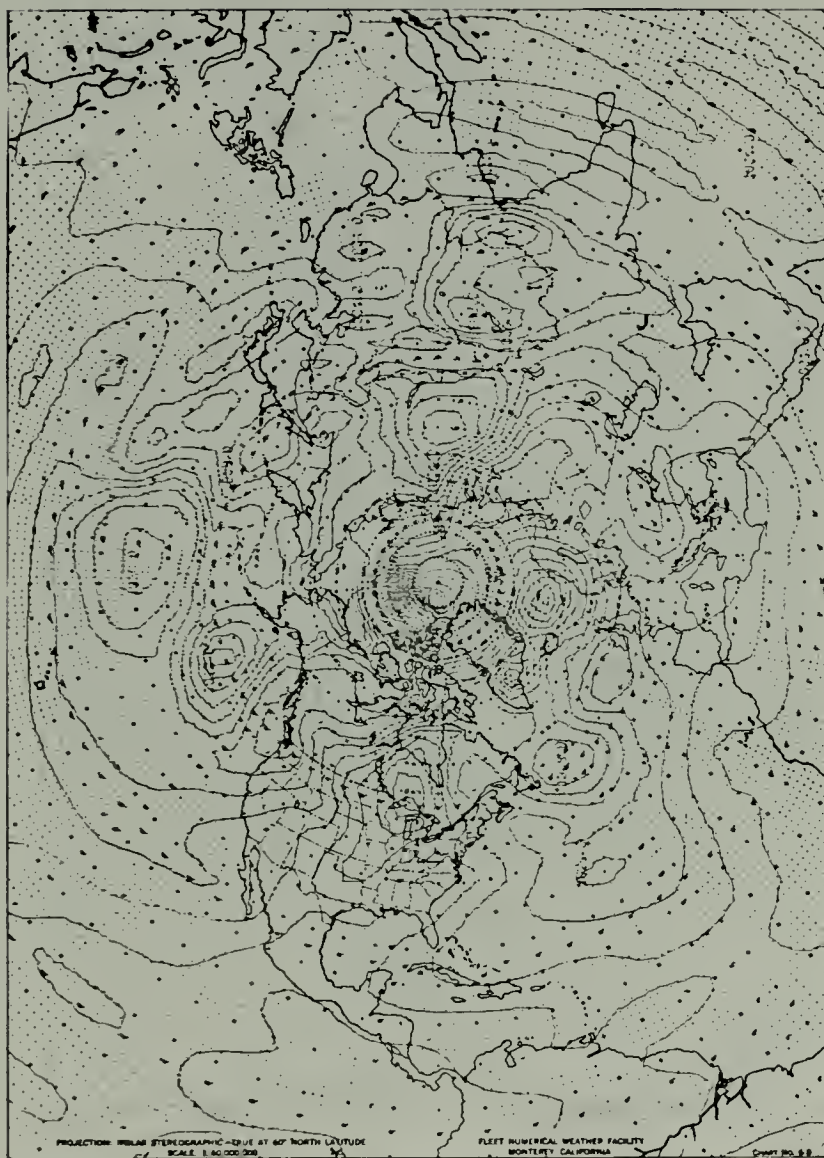


Chart D. 36-Hour Forecast, Second Order Scheme.



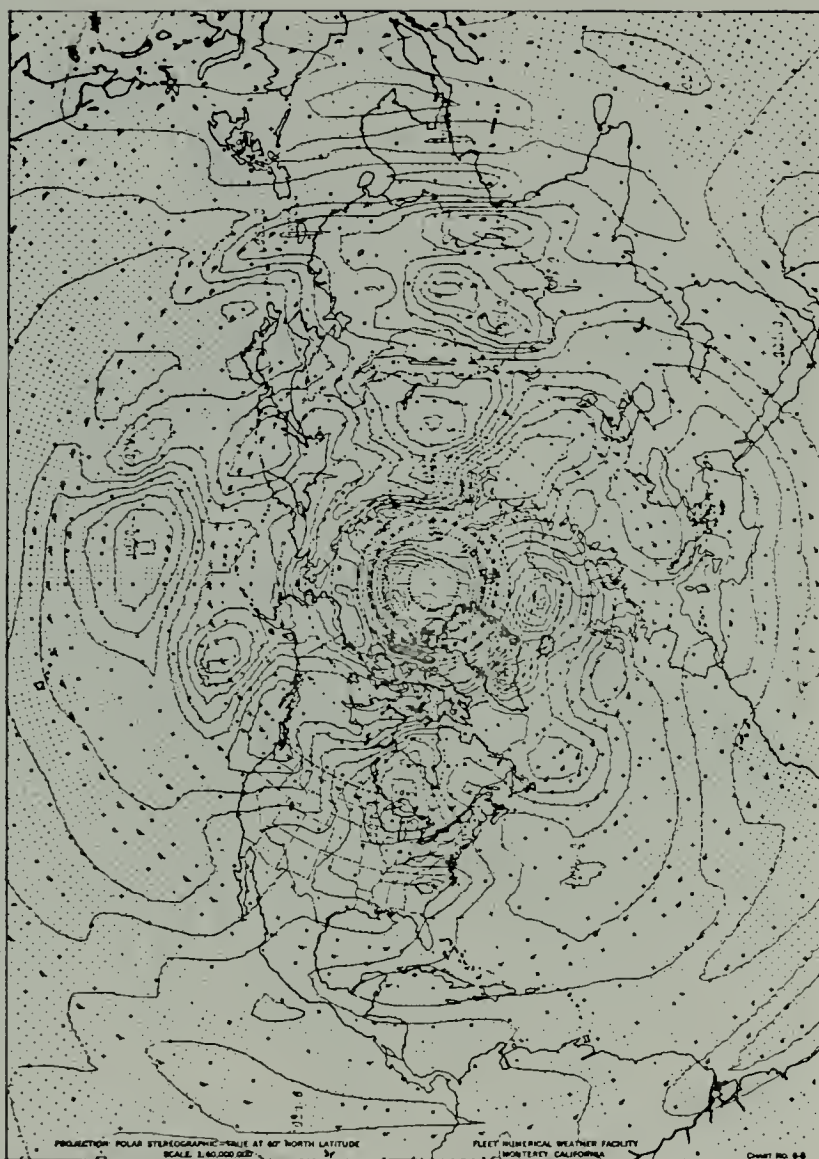


Chart E. 48-Hour Forecast, Second Order Scheme.











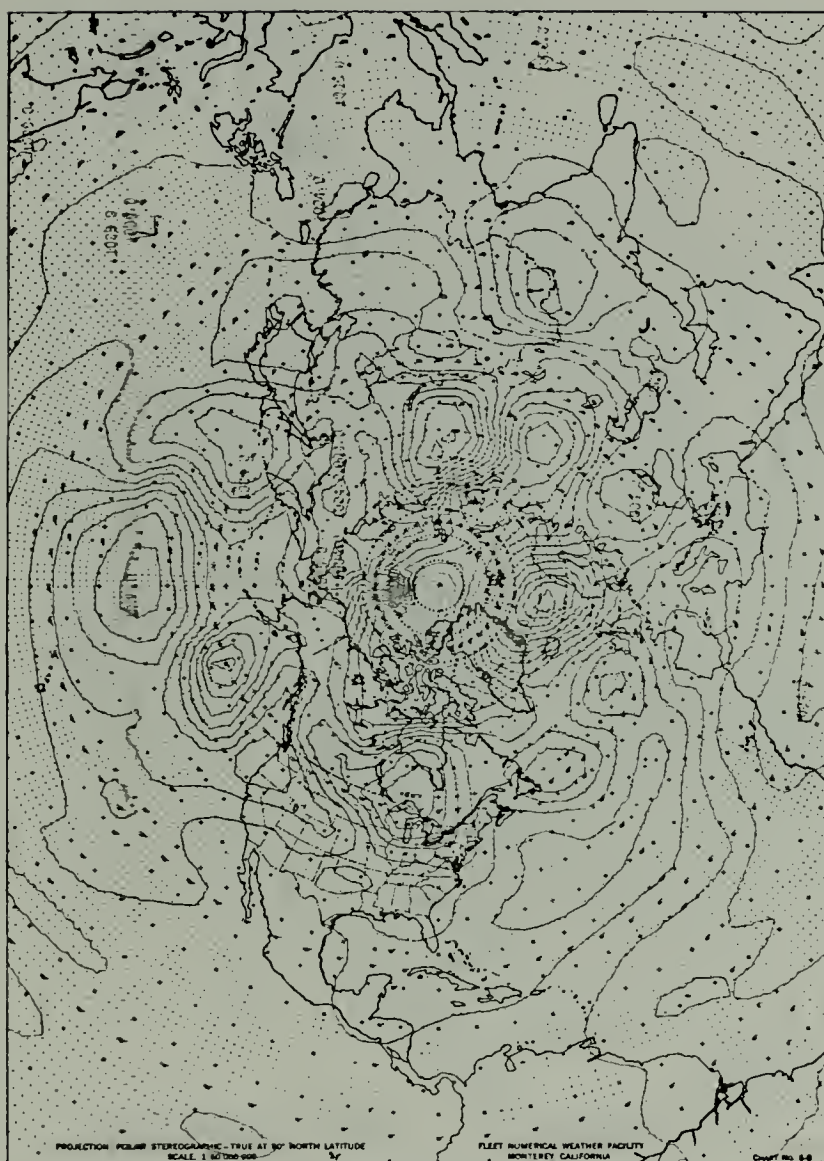


Chart G. 24-Hour Forecast, Mixed Scheme.



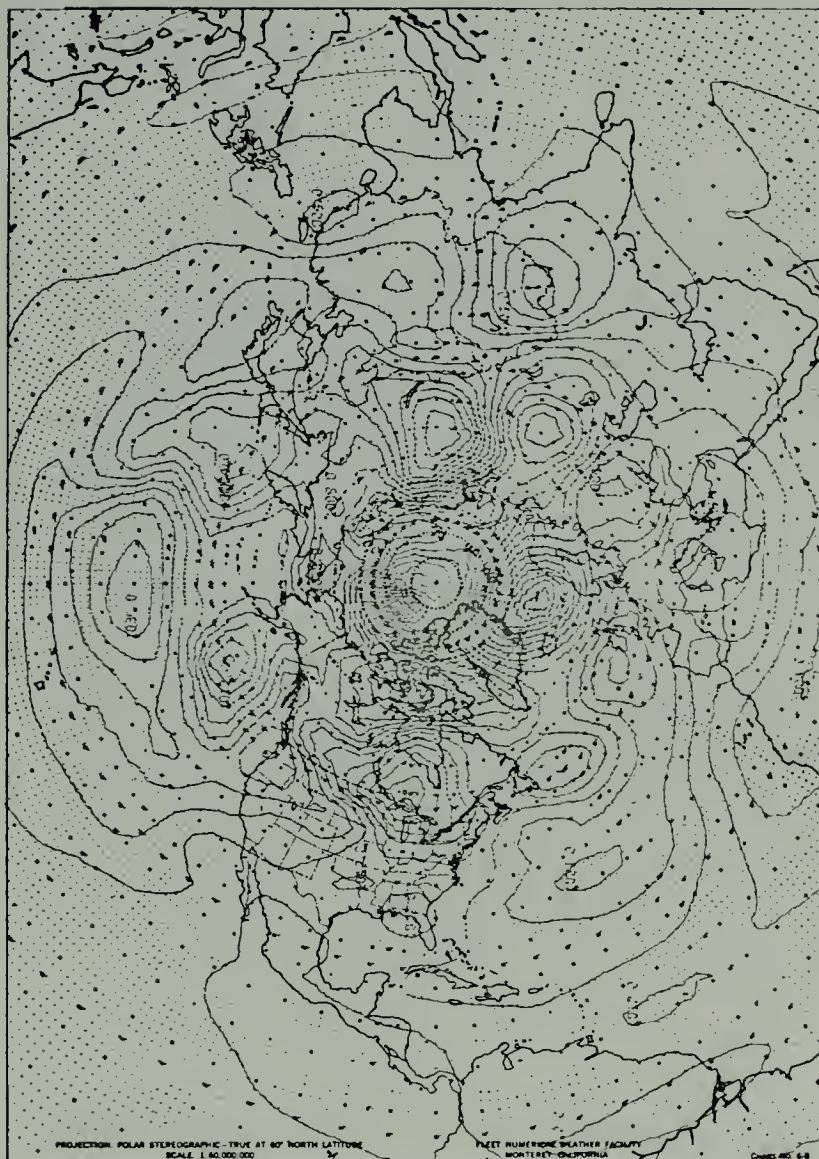


Chart H. 36-Hour Forecast, Mixed Scheme.



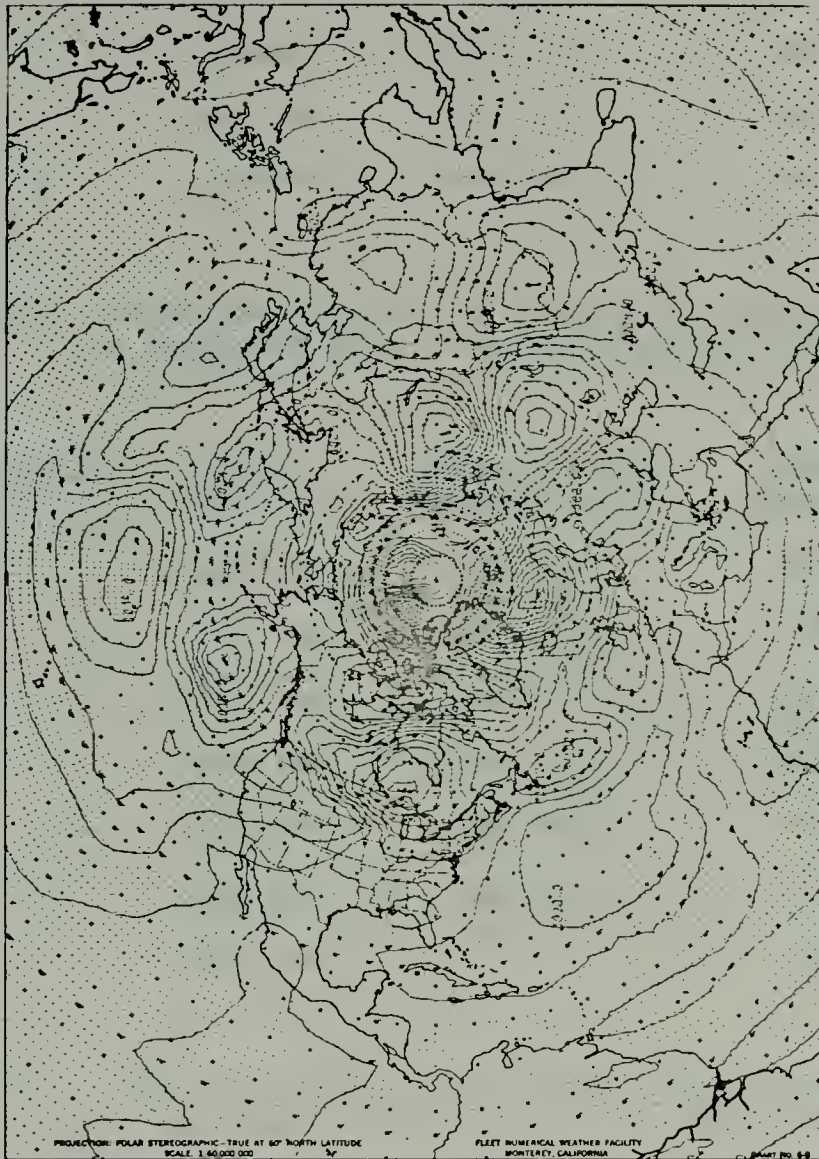


Chart I. 48-Hour Forecast, Mixed Scheme.



HIGH CENTER NUMBER	INITIAL POSITION	48-HOUR SECOND ORDER POSITION	48-HOUR MIXED SCHEME POSITION
1	37N 177W	37N 177W	35N 172W
2	35N 136W	47N 128W	43N 121W
3	None	31N 53W	33N 48W
4	45N 25W	52N 17W	52N 12W
5	64N 50E	60N 60E	52N 66W

TABLE II. Initial Positions of High Centers and Forecast Positions of the Second Order Scheme and the Mixed Scheme.

LOW CENTER NUMBER	INITIAL POSITION	48-HOUR SECOND ORDER POSITION	48-HOUR MIXED SCHEME POSITION
1	47N 155W	48N 152W	49N 147W
2	47N 89W	50N 45W	48N 40W
3	47N 50W	50N 87W	51N 88W
4	67N 02E	68N 03E	68N 04E
5	61N 89E	59N 99E	61N 97E
6	36N 152E	50N 151E	48N 160E
7	30N 80E	*	33N 81E

TABLE III. Initial Positions of Low Centers and Forecast Positions of the Second Order Scheme and the Mixed Scheme.

\*Several small lows were forecast by the second order scheme.





## VI. CONCLUSIONS

Both the analytic and real data experiments indicate that the mixed fourth and second order differencing scheme gives a more accurate solution for the meteorological phase speeds. More analytic experiments with a more realistic phase speed will have to be performed to produce the final conclusive proof of the mixed scheme. A series of real data experiments should also be considered. In addition the fourth order differencing must eventually be extended to the poles.



APPENDIX A  
DIFFERENCE EQUATIONS

The longitudinal momentum equation terms in difference form are:

$$\frac{\partial u\pi}{\partial t} \equiv \frac{\pi u_{ij}^{n+1} - \pi u_{ij}^{n-1}}{2\Delta t}, \quad (1)$$

$$\begin{aligned} & - \frac{1}{a \cos \theta} \left[ \frac{\partial(uu\pi)}{\partial \lambda} + \frac{\partial(uv\pi) \cos \theta}{\partial \theta} \right] \equiv \\ & - \frac{1}{a \cos \theta_j} \left[ \frac{(u_{ij} + u_{i+1,j}) \overline{u\pi}_{i+1/2,j} - (u_{ij} + u_{i-1,j}) \overline{u\pi}_{i-1/2,j}}{2\Delta \lambda} \right. \\ & \left. + \frac{(u_{ij} + u_{i,j+2}) \overline{v\pi}_{i,j+1} \cos \theta_{j+1} - (u_{ij} + u_{i,j-2}) \overline{v\pi}_{i,j-1} \cos \theta_{j-1}}{2\Delta \theta} \right] \quad (2) \end{aligned}$$

where

$$\overline{u\pi}_{i+1/2,j} \equiv \frac{1}{4} (\pi_{ij} u_{ij} + \pi_{i+1,j} u_{i+1,j} + \pi_{i,j+1} u_{i,j+1} + \pi_{i,j-1} u_{i,j-1}), \quad (2.1)$$

$$\begin{aligned} \overline{u\pi}_{i-1/2,j} \equiv \frac{1}{4} (\pi_{ij} u_{ij} + \pi_{i-1,j} u_{i-1,j} + \pi_{i-1,j+1} u_{i-1,j+1} + \\ \pi_{i-1,j-1} u_{i-1,j-1}) \quad (2.2) \end{aligned}$$

$$\begin{aligned} \overline{u\pi}_{i,j+1} \equiv \frac{1}{4} (\pi_{ij} u_{ij} + \pi_{i,j+2} u_{i,j+2} + \pi_{i-1,j+1} u_{i-1,j+1} + \\ \pi_{i,j-1} u_{i,j-1}) \quad (2.3) \end{aligned}$$



$$\overline{u\pi}_{i,j-1} \equiv \frac{1}{4}(\overline{\pi}_{ij}u_{ij} + \overline{\pi}_{i,j-2}u_{i,j-2} + \overline{\pi}_{i-1,j-1}u_{i-1,j-1} + \overline{\pi}_{i,j-1}u_{i,j-1}) \quad (2.4)$$

The longitudinal grid increment ( $\Delta\lambda$ ) and the latitudinal grid increment ( $\Delta\theta$ ) are both ten degrees.

$$\pi \frac{\partial w u}{\partial \sigma} \equiv \overline{\pi}_{ij} \left[ \frac{w_{ijk}(u_{ij,k+1} + u_{ijk})}{2\Delta\sigma} - \frac{w_{ij,k-1}(u_{ijk} + u_{ij,k-1})}{2\Delta\sigma} \right] \quad (3)$$

where the vertical velocity,  $-\dot{\sigma}$ , is defined as,

$$w_{k+1} \equiv w_{ijk} - \frac{\Delta\sigma}{\overline{\pi}_{ij}} \left[ \left( \frac{\partial \pi}{\partial t} \right)_{ij}^N + \frac{1}{a \cos \theta_j} \left[ \frac{u_{i+1,jk} - u_{i+1,jk} - u_{ijk}}{\Delta\lambda} + \frac{v_{ij+1k} \cos \theta_{j+1} - v_{ij-1k} \cos \theta_{j-1}}{\Delta\theta} \right] \right] \quad (4)$$

and the local change as

$$\left( \frac{\partial \pi}{\partial t} \right)_{ij}^N \equiv \sum_{k=1}^5 \left[ \frac{u_{i+1,jk} - u_{ijk}}{\Delta\lambda a \cos \theta_j} + \frac{v_{ij+1k} \cos \theta_{j+1} - v_{ij-1k} \cos \theta_{j-1}}{\Delta\theta a \cos \theta_j} \right] \quad (5)$$

The  $u\overline{\pi}$  terms of Equations (4) and (5) are,

$$u\overline{\pi}_{i+1j} = u_{i+1j} (\pi_{ij} + \pi_{i+1j} + \pi_{ij+1} + \pi_{ij-1}) \frac{1}{4} \quad (5.1)$$

The quantities  $u\overline{\pi}_{ij}$ ,  $u\overline{\pi}_{ij+1}$  and  $u\overline{\pi}_{ij-1}$  are also determined in the same manner.



$$\pi v f \equiv f_j \bar{\pi}_{ij} u_{ij} \quad (6)$$

where

$$\bar{\pi}_{ij} = \frac{1}{4}(\pi_{ij} + \pi_{i-1j} + \pi_{i-1,j+1} + \pi_{i-1,j-1}) \quad (6.1)$$

$$\frac{\pi_{uv} \tan \theta}{a} = \frac{u_{ij} (\bar{\pi}_{ij}) \tan \theta_j}{a} \quad (7)$$

$$\begin{aligned} & - \frac{1}{a \cos \theta} \left[ RT \frac{\partial \pi}{\partial \lambda} + \pi \frac{\partial \Phi}{\partial \lambda} \right] \equiv \\ & - \frac{1}{a \cos \theta_j} \left[ R \bar{T}_{ij} \left( \frac{\partial \pi}{\partial \lambda} \right)^* + \bar{\pi}_{ij} \frac{(\Phi_{ij} - \Phi_{i-1,j})}{\Delta \lambda} \right] \end{aligned} \quad (8)$$

where

$$\bar{T}_{ij} \equiv \frac{1}{4}(T_{i-1j} + T_{ij} + T_{i-1,j+1} + T_{i-1,j-1}) \quad (8.1)$$

$$\bar{\pi}_{ij} \equiv \frac{1}{4}(\pi_{i-1j} + \pi_{ij} + \pi_{i-1,j+1} + \pi_{i-1,j-1}) \quad (8.2)$$

From Equation (9) of section II the change of terrain height is found as follows

$$\left( \frac{\partial \pi}{\partial \lambda} \right)^*_{\sigma} = \frac{\pi}{RT} \left[ \frac{(\Phi_R - \Phi_L)}{\Delta \lambda} p - \frac{(\Phi_R - \Phi_L)}{\Delta \lambda} \sigma \right] \quad (9)$$

$$= \frac{\pi}{RT} \left[ \frac{(\Phi_R - \Phi_L)_p + (\Phi_L - \Phi_L)_\sigma}{\Delta \lambda} \right] \quad (10)$$





where  $\phi_R$  is to the right of the computational point and  $\phi_L$  is to the left of the computational point. Sigma and p indicate the surface in question. The thickness between the pressure surface and the sigma surface to the right and left of the computational point is defined as,

$$\Delta\phi_{R_{\sigma p}} = (\phi_{R_p} - \phi_{R_{\sigma}}) \quad \text{and} \quad (11)$$

$$\Delta\phi_{L_{\sigma p}} = (\phi_{L_{\sigma}} - \phi_{L_p}) \quad (12)$$

therefore one can write,

$$\Delta\phi_{R_{\sigma p}} = -R\bar{T}_{\sigma p} \ln \frac{p_1}{p_2} \quad (13)$$

$$\Delta\phi_{L_{\sigma p}} = -R\bar{T}_{\sigma p} \ln \frac{p_1}{p_2} \quad (14)$$

The mean temperature is found as follows,

$$\bar{T} = T_{\text{comp}} + \frac{\partial T}{\partial \sigma} \left[ \frac{\Delta \ln \pi}{2} \right] \quad (15)$$

and in difference form

$$\bar{T}_{R_{\sigma p}} = \bar{T}_{ij} + \frac{(T_{R_{\sigma+1}} - T_{R_{\sigma}})}{\Delta\sigma} \frac{(\ln \bar{\pi}_{ij} - \ln \pi_{ij})}{2} \quad (16)$$

$$\bar{T}_{L_{\sigma p}} = \bar{T}_{ij} + \frac{(T_{L_{\sigma+1}} - T_{L_{\sigma}})}{\Delta\sigma} \frac{(\ln \bar{\pi}_{ij} - \ln \pi_{ij})}{2} \quad (17)$$



$$\bar{T}_{ij} = \frac{1}{4}(T_{ij} + T_{i-1j} + T_{i-1,j+1} + T_{i-1,j-1}) \quad (17.1)$$

$$\text{LN } \bar{\pi}_{ij} = \frac{1}{4}(\text{ln } \pi_{ij} + \text{ln } \pi_{i-1j} + \text{ln } \pi_{i-1,j+1} + \text{ln } \pi_{i-1,j-1}) \quad (17.2)$$

Figure 5 illustrates the differencing in both the horizontal and vertical. Substituting Equations (16) and (17) into Equations (13) and (14) one obtains,

$$\Delta\Phi_{R_{\sigma p}} = -R[\bar{T}_{ij} + \frac{(T_{R_{\sigma+1}} - T_{R_{\sigma}})}{\Delta\sigma} \frac{(\text{ln } \bar{\pi}_{ij} - \text{ln } \pi_{ij})}{2}] - (\text{ln } \bar{\pi}_{ij} - \text{ln } \pi_{ij}) \quad (18)$$

$$\Delta\Phi_{L_{\sigma p}} = -R[\bar{T}_{ij} + \frac{(T_{L_{\sigma+1}} - T_{L_{\sigma}})}{\Delta\sigma} \frac{(\text{ln } \bar{\pi}_{ij} - \text{ln } \pi_{i-1j})}{2}] - \text{ln } \bar{\pi}_{ij} - \text{ln } \pi_{i-1j} \quad (19)$$

where

$$\text{ln}_R \frac{p_1}{p_{\sigma+1}} = \text{ln} \frac{(\sigma_{+1} \Delta\pi)}{\sigma_{+1} \pi} = \text{ln } \bar{\pi}_{ij} - \text{ln } \pi_{ij} \quad (20)$$

and

$$\text{ln}_L \frac{p_1}{p_{\sigma+1}} = \text{ln } \bar{\pi}_{ij} - \text{ln } \pi_{i-1j} \quad (21)$$



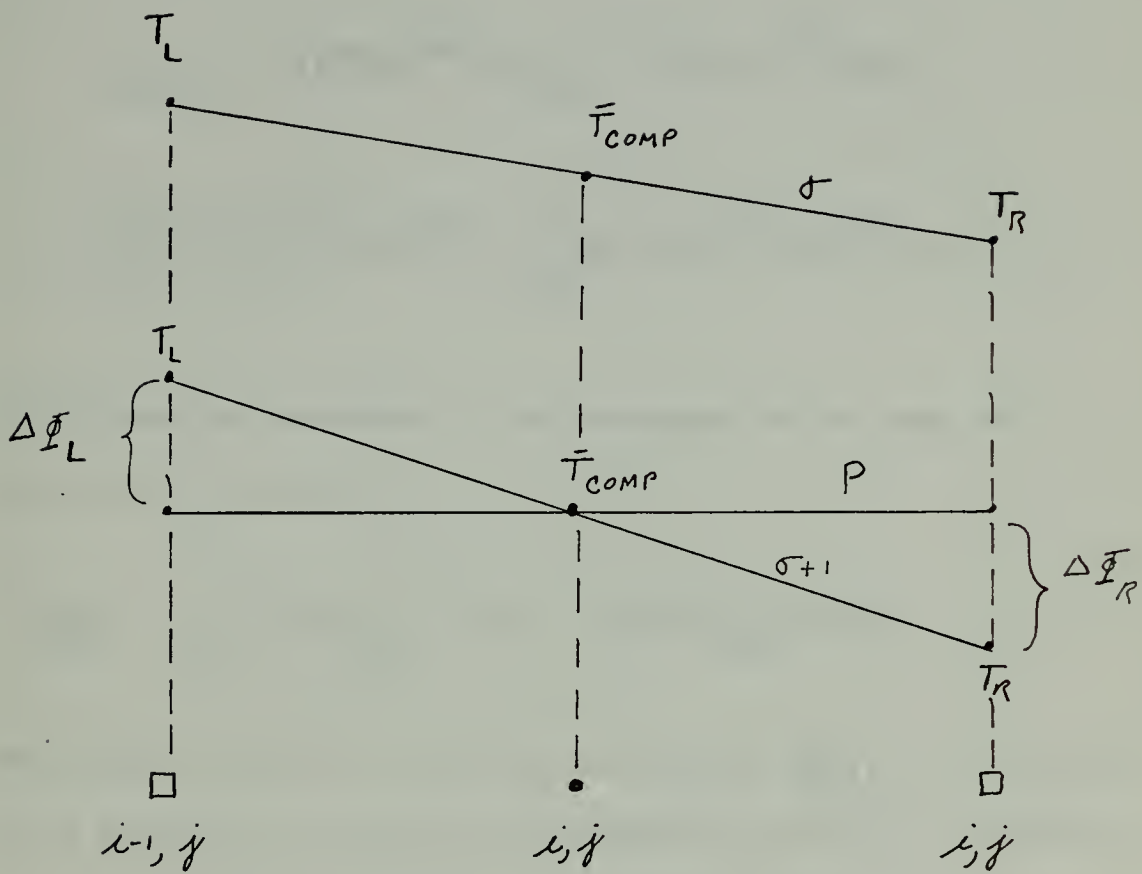


Figure 5. Interpolation for  $\nabla\pi$ .



The latitudinal-momentum equation terms in difference form are,

$$\frac{\partial v\pi}{\partial t} \equiv \frac{\pi v_{ij}^{N+1} - \pi v_{ij}^{N-1}}{2\Delta t} \quad (1)$$

$$\begin{aligned} & - \frac{1}{a \cos \theta} \left[ \frac{\partial(\pi v w)}{\partial \lambda} + \frac{\partial(\pi v v \cos \theta)}{\partial \theta} \right] \equiv \\ & - \frac{1}{a \cos \theta_j} \left[ \frac{(v_{ij} + v_{i+1j}) \overline{u\pi}_{i+1/2j} - (v_{ij} + v_{i-1j}) \overline{u\pi}_{i-1/2j}}{2\Delta \lambda} \right. \\ & \left. + \frac{(v_{ij} + v_{ij+2}) \overline{v\pi}_{ij+1} \cos \theta_{j+1} - (v_{ij} - v_{ij-2}) \overline{v\pi}_{ij-1} \cos \theta_{j-1}}{2\Delta \theta} \right] \quad (2) \end{aligned}$$

The  $\overline{u\pi}$  terms are determined in the same manner as the terms for Equation (2) were found.

$$\frac{\pi \partial(wv)}{\partial \sigma} = \overline{\pi}_{ij} \left[ \frac{w_{\sigma} (v_{ij\sigma+1} + v_{ij\sigma})}{2\Delta \sigma} - \frac{w_{\sigma-1} (v_{ij\sigma} + v_{ij\sigma-1})}{2\Delta \sigma} \right] \quad (3)$$

The vertical velocity,  $w$ , and the local change,  $(\frac{\partial \pi}{\partial t})_{ij}^n$ , are obtained as in Equations (4) and (5) of the longitudinal equation of momentum.

$$\pi v f = f_j \overline{\pi}_{ij} v_{ij} \quad (4)$$

$\overline{\pi}_{ij}$  = Equation (6.1) or the  $u$ -equation of momentum +

$$\frac{\overline{\pi} u u \tan \theta}{a} \equiv \frac{u_{ij} (\overline{\pi}_{ij} u_{ij}) \tan \theta_j}{a} \quad (5)$$





$$- \frac{1}{a} \left[ \pi \frac{\partial \phi}{\partial \theta} + RT \frac{\partial \pi}{\partial \theta} \right] \equiv$$

$$- \frac{1}{a \cos \theta_j} \left[ RT_{ij} \left( \frac{\partial \pi}{\partial \theta} \right)^*_{\sigma} + \bar{\pi}_{ij} \frac{(\phi_{i-1,j+1} - \phi_{i-1,j-1})}{\Delta \theta} \right] \quad (6)$$

$$\left( \frac{\partial \pi}{\partial \theta} \right)^*_{\sigma} = \frac{\pi}{RT} \left[ \frac{(\phi_{R_p} - \phi_{R_{\sigma}}) + (\phi_{L_{\sigma}} - \phi_{L_p})}{\Delta \theta} \right] \quad (7)$$

Equation (7) is solved by the same method as was shown for the longitudinal momentum equation.

#### Thermodynamic Equation

$$\frac{\partial (\pi T)}{\partial t} \equiv \frac{\pi T_{ij\sigma}^{N+1} - \pi T_{ij\sigma}^{N-1}}{2\Delta t} \quad (1)$$

$$\frac{1}{a \cos \theta} \left[ \frac{\partial (\pi u T)}{\partial \lambda} + \frac{\partial (\pi v T \cos \theta)}{\partial \theta} \right] \equiv$$

$$\frac{1}{a \cos \theta_j} \left[ \frac{\bar{T}_{i+1j} (u_{i+1j} \bar{\pi}_{i+1j}) - \bar{T}_{ij} (u_{ij} \bar{\pi}_{ij})}{\Delta \lambda} \right.$$

$$\left. \frac{\bar{T}_{ij+1} (v_{ij+1} \bar{\pi}_{ij+1}) \cos \theta_{j+1} + \bar{T}_{ij-1} v_{ij-1} \bar{\pi}_{ij-1} \cos \theta_{j-1}}{\Delta \theta} \right] \quad (2)$$

where  $\bar{T}$  is the temperature at the velocity point based on the average of the four surrounding mass points and  $\bar{\pi}$  is also calculated in the same manner.



$$\pi \frac{\partial(wT)}{\partial \sigma} = \pi_{ij} \left[ \frac{w_{ij\sigma} (T_{ij\sigma+1} + T_{ij\sigma})}{2\Delta\sigma} - \frac{w_{ij\sigma-1} (u_{ij\sigma} + u_{ij\sigma-1})}{2\Delta\sigma} \right] \quad (3)$$

The vertical velocity,  $w$ , and the local change,  $(\frac{\partial \pi}{\partial t})^N_y$ , are obtained as in the  $u$ -equation of motion.

$$\frac{RT}{c_p \sigma} \left[ -w\pi + \sigma \left( \frac{\partial \pi}{\partial t} + \frac{1}{a \cos \theta} [u \frac{\partial \pi}{\partial \lambda} + v \frac{\partial \pi}{\partial \theta} \cos \theta] \right) \right] \equiv$$

$$\frac{RT}{c_p \sigma} \left[ \frac{(w_\sigma + w_{\sigma-1})}{2} \pi_{ij} + \sigma_\sigma \left( \frac{\partial \pi}{\partial t} \right)_{ij} + \right.$$

$$\left. \frac{\sigma_\sigma}{a \cos \theta_j} \left[ \frac{(u_{i+1j} \bar{\pi}_{i+1j} - u_{ij} \bar{\pi}_{ij})}{2\Delta\lambda} + \right. \right.$$

$$\left. \left. \frac{(v_{ij+1} \bar{\pi}_{ij+1} \cos \theta_{j+1} - v_{ij-1} \bar{\pi}_{ij-1} \cos \theta_{j-1})}{2\Delta\theta} \right] \right] \quad (4)$$

where the vertical velocity and the local change are again computed as before.

The Moisture Equation

$$\frac{\partial q \pi}{\partial t} \equiv \frac{q \pi_{ij}^{N+1} - q \pi_{ij}^{N-1}}{2\Delta t} \quad (1)$$

$$\begin{aligned} & - \frac{1}{a \cos \theta} \left[ \frac{\partial u \pi q}{\partial \lambda} + \frac{\partial (v \pi q \cos \theta)}{\partial \theta} \right] \equiv \\ & - \frac{1}{a \cos \theta_j} \left[ \frac{\bar{q}_{i+1j} (u_{i+1j} \bar{\pi}_{i+1j}) - \bar{q}_{ij} (u_{ij} \bar{\pi}_{ij})}{\Delta \lambda} + \right. \\ & \left. \frac{\bar{q}_{ij+1} (v_{ij+1} \bar{\pi}_{ij+1} \cos \theta_{j+1}) - \bar{q}_{ij-1} (v_{ij-1} \bar{\pi}_{ij-1} \cos \theta_{j-1})}{\Delta \sigma} \right] \end{aligned} \quad (2)$$



where  $\bar{q}$  is the specific humidity at the velocity point based on the average of the four surrounding mass points and  $\bar{\pi}$  is also calculated in the same manner.

$$\pi \frac{\partial(wq)}{\partial\sigma} = \pi_{ij} \left[ \frac{w_{ij\sigma}(q_{ij\sigma+1} + q_{ij\sigma})}{2\Delta\sigma} - \frac{w_{ij\sigma-1}(u_{ij\sigma} + u_{ij\sigma-1})}{2\Delta\sigma} \right] \quad (3)$$

The Hydrostatic Equation

$$d\phi = - RT \, d\ln \sigma$$

$$\phi_{k+1} = \phi_k - R \ln \frac{\sigma_{k+1}}{\sigma_k} \left[ \frac{T_k \ln\left(\frac{\sigma_k}{\pi}\right) + T_{k+1} \ln\left(\frac{\sigma_{k+1}}{\pi}\right)}{\ln\sigma_k + \ln\sigma_{k+1} - 2\ln\pi} \right]$$

At the lowest level  $\phi$  is given as

$$\phi_{ij} = \pi - RT_{ijk} \ln (0.9)$$



## APPENDIX B

In accordance with the work of Williams (1972) the fourth order terms are a sum of a weighted average of the second order and fourth order differencing. The weighting factor the second order part is four-thirds and a minus one-third for the fourth order portion. The advection term of the longitudinal momentum equation is:

$$\begin{aligned}
 & - \frac{1}{a \cos \theta_j} \left[ \frac{4}{3} \left\{ \frac{(u_{ij} + u_{i+1j}) \overline{u\pi}_{i-1/2j} - (u_{ij} + u_{i-1j}) \overline{u\pi}_{i-1/2j}}{2\Delta\lambda} \right. \right. \\
 & + \frac{(u_{ij} + u_{ij+2}) \cos \theta_{j+1} \overline{v\pi}_{ij+1} - (u_{ij} + u_{ij-2}) \cos \theta_{j-1} \overline{v\pi}_{ij-1}}{2\Delta\lambda} \\
 & - \frac{1}{3} \left\{ \frac{(u_{ij} + u_{i+2j}) \overline{u\pi}_{i+1j} - (u_{ij} + u_{i-2j}) \overline{u\pi}_{i-1j}}{4\Delta\lambda} \right. \\
 & \left. \left. + \frac{(u_{ij} + u_{ij+4}) \cos \theta_{j+2} \overline{v\pi}_{ij+2} - (u_{ij} + u_{ij-4}) \cos \theta_{j-2} \overline{v\pi}_{ij-2}}{4\Delta\lambda} \right\} \right] \quad (1)
 \end{aligned}$$

The  $\overline{v\pi}$  terms are determined as shown in Appendix A. The advection term for the latitudinal momentum equation is similar to term (1). The advection term of the thermodynamic equation is:

$$\begin{aligned}
 & - \frac{1}{a \cos \theta_j} \left[ \frac{4}{3} \left\{ \frac{\overline{T}_{i+1j} \overline{u\pi}_{i+1j} - \overline{T}_{ij} \overline{u\pi}_{ij}}{\Delta\lambda} \right. \right. \\
 & \left. \frac{\overline{T}_{ij+1} \overline{u\pi}_{ij+1} \cos \theta_{j+1} - \overline{T}_{ij-1} \overline{u\pi}_{ij-1} \cos \theta_{j-1}}{\Delta\lambda} \right\} \\
 & - \frac{1}{3} \left\{ \frac{\overline{T}_{i+1j}^* \overline{u\pi}_{i+1j}^* - \overline{T}_{i-1j}^* \overline{u\pi}_{i-1j}^*}{2\Delta\lambda} + \right. \\
 & \left. \frac{\overline{T}_{ij+2}^* \overline{u\pi}_{ij+2}^* \cos \theta_{j+2} - \overline{T}_{ij-2}^* \overline{u\pi}_{ij-2}^* \cos \theta_{j-2}}{2\Delta\theta} \right\} \right] \quad (2)
 \end{aligned}$$





The program as written gives the average temperatures,  $\bar{T}$ , and  $\bar{u}_\pi$  values at velocity points for the second order differencing. For fourth order differencing the grid distance is doubled and the values  $\bar{T}^*$  and  $\bar{u}_\pi^*$  are determined at the adjacent mass points. All the averaged quantities are determined similarly to those in Appendix A.

The flux term of the continuity equation is:

$$\begin{aligned} & \frac{1}{a \cos \theta_j} \left[ \frac{4}{3} \left\{ \frac{\bar{u}_\pi^{i+1jk} - \bar{u}_\pi^{ijk}}{\Delta \lambda} + \right. \right. \\ & \frac{\bar{v}_\pi^{ij+1k} \cos \theta_{j+1} - \bar{v}_\pi^{ij-1k} \cos \theta_{j-1}}{\Delta \lambda} \left. \right\} \\ & - \frac{1}{3} \left\{ \frac{\bar{u}_\pi^{*i+1jk} - \bar{u}_\pi^{*i-1jk}}{2\Delta \lambda} + \right. \\ & \left. \left. \frac{\bar{v}_\pi^{*ij+2k} \cos \theta_{j+2} - \bar{v}_\pi^{*ij-2k} \cos \theta_{j-2}}{2\Delta \theta} \right\} \right] \end{aligned}$$

The averaged values are also determined as indicated in Appendix A. The unstarred quantities are at a velocity point and the starred quantities are at a mass point. For this experiment the fourth order differencing was blended with the second order differencing at 75° latitude. This was done to avoid having to go over the poles to pick up the  $j+1$ ,  $j+2$  and  $j+3$  quantities at the higher latitudes.



## LIST OF REFERENCES

1. Arakawa, Akio, Katayama, Akira, and Mintz, "Numerical Simulation of the General Circulation of the Atmosphere," Proceedings of the WMO/IUGG Symposium on Numerical Weather Prediction, Tokyo, Japan, November 26 - December 4, 1968, Japan Meteorological Agency, Tokyo, March 1969, pp. IV-1 - IV-4.
2. Arakawa, Akio, "Computational Design for Long-Term Numerical Integration of the Equations of Fluid Motion: Two Dimensional Incompressible Flow. Part I," Journal of Computational Physics, Vol. 1, No. 1, Academic Press, Inc., New York, N.Y., January 1966, pp. 119-143.
3. Dickson, Robert R., and Posey, Julian, "Maps of Snow-Cover Probability for the Northern Hemisphere," Monthly Weather Review, Vol. 95, No. 6, June 1965, p. 347-353.
4. Gates, W. L., "On the Truncation Error, Stability and Convergence of Difference Solutions of the Barotropic Vorticity Equation," J. Meteor., v. 16, p. 556-568, 1959.
5. Gates, W. L., and Riegel, C. A., "A Study of Numerical Errors in the Integration of Barotropic Flow on a Spherical Grid," J. of Geoph. Res., v. 67, No. 2, p. 773-784, February 1962.
6. Haltiner, G. J., Numerical Weather Prediction, p. 1-39, 90-114, 193-196 and 220-243, Wiley, 1971.
7. Haltiner, G. J., and Martin, F. L., Dynamical and Physical Meteorology, p. 52-53, McGraw-Hill, 1957.
8. Haurwitz, B., 1940: The Motion of Atmospheric Disturbances. J. Marine Research (Sears Foundation), v. 3, p. 35-50.
9. Haurwitz, B., 1940: The Motion of Atmospheric Disturbances on the Spherical Earth. J. Marine Research (Sears Foundation), v. 3, p. 254-267.
10. Heburn, G. W., Numerical Experiments with Several Time Differencing Schemes with a Barotropic Primitive Equation Model on a Spherical Grid, M. S. Thesis, Naval Postgraduate School, 1972.
11. Holton, J. R., An Introduction to Dynamic Meteorology, p. 179-181, Academic Press, 1972.
12. Kesel and Winninghoff, "The Fleet Numerical Weather Central Operational Primitive-Equation Model," Monthly Weather Review, v. 100, No. 5, p. 360-373, 1972.



13. Kreyszig, E., Advanced Engineering Mathematics, p. 175-178, Wiley, 1962.
14. Naval Postgraduate School Report NPS-51Wu72031A, Phase Speed Errors with Second and Fourth Order Space Differences with Staggered and Unstaggered Grids, by R. T. Williams, March 1972.
15. Naval Postgraduate School Report NPS-51Wu71081A, Restorative Iterative Initialization for a Global Prediction Model, by F. J. Winninghoff, September 1971.
16. Neamtan, S. M., "The Motion of Harmonic Waves in the Atmosphere," J. Meteorology, v. 3, p. 53-56, 1946.
17. UCLA Department of Meteorology Technical Report No. 3, Description of the Mintz-Arakawa Numerical General Circulation Model, by W. E. Langlois and C. W. Kwok, 1969.
18. Smagorinsky et al., "Numerical Results from a Nine-Level General Circulation Model of the Atmosphere," Monthly Weather Review, v. 93, No. 12, December 1965, pp. 727-768.



INITIAL DISTRIBUTION LIST

	No. Copies
1. Defense Documentation Center Cameron Station Alexandria, Virginia 22314	2
2. Library, Code 0212 Naval Postgraduate School Monterey, California 93940	2
3. Dr. George J. Haltiner Chairman, Department of Meteorology Naval Postgraduate School Monterey, California 93940	5
4. Associate Professor Roger T. Williams Code 51 Department of Meteorology Naval Postgraduate School Monterey, California 93940	5
5. Lieutenant William T. Elias Fleet Numerical Weather Central Naval Postgraduate School Monterey, California 93940	1
6. Officer in Charge Environmental Prediction Research Facility Naval Postgraduate School Monterey, California 93940	1
7. Commanding Officer Fleet Numerical Weather Central Naval Postgraduate School Monterey, California 93940	1
8. LCDR Wayne R. Lambertson Fleet Numerical Weather Central Naval Postgraduate School Monterey, California 93940	1
9. ARCRL - Research Library L. G. Hanscom Field Attn: Nancy Davis/Stop 29 Bedford, Massachusetts 01730	1
10. Director, Naval Research Laboratory Attn: Tech. Services Info. Officer Washington, D. C. 20390	1





11. American Meteorological Society 1  
45 Beacon Street  
Boston, Massachusetts 02128
12. Department of Meteorology, Code 51 3  
Naval Postgraduate School  
Monterey, California 93940
13. Department of Oceanography, Code 58 1  
Naval Postgraduate School  
Monterey, California 93940
14. Office of Naval Research 1  
Department of the Navy  
Washington, D. C. 20360
15. Commander, Air Weather Service 2  
Military Airlift Command  
U. S. Air Force  
Scott Air Force Base, Illinois 62226
16. Atmospheric Sciences Library 1  
National Oceanic and Atmospheric Administration  
Silver Spring, Maryland 20910
17. National Center for Atmospheric Research 1  
Box 1470  
Boulder, Colorado 80302
18. Dr. T. N. Krishnamurti 1  
Department of Meteorology  
Florida State University  
Tallahassee, Florida 32306
19. Dr. Fred Shuman, Director 1  
National Meteorological Center  
Environmental Science Services Administration  
Suitland, Maryland 20390
20. Dr. J. Smagorinsky, Director 1  
Geophysical Fluid Dynamics Laboratory  
Princeton University  
Princeton, New Jersey 08540
21. Dr. A. Arakawa 1  
Department of Meteorology  
UCLA  
Los Angeles, California 90024
22. Professor N. A. Phillips, 54-1422 1  
M.I.T.  
Cambridge, Massachusetts 02139



23. Dr. Russell Elsberry 1  
Department of Meteorology  
Naval Postgraduate School  
Monterey, California 93940
24. Dr. Jerry D. Mahlman 1  
Geophysical Fluid Dynamics Laboratory  
Princeton University  
Princeton, New Jersey 08540
25. Dr. Robert L. Haney 1  
Department of Meteorology  
Naval Postgraduate School  
Monterey, California 93940
26. Dr. Ron L. Alberty 1  
National Severe Storm Laboratory  
1616 Halley Circle  
Norman, Oklahoma 73069
27. Dr. W. L. Gates 1  
The RAND Corporation  
1700 Main Street  
Santa Monica, California 90406
28. Dr. Richard Alexander 1  
The RAND Corporation  
1700 Main Street  
Santa Monica, California 90406
29. Commanding Officer 1  
Fleet Weather Central  
Box 110  
FPO San Francisco, California 96610
30. Dr. F. J. Winninghoff 1  
Department of Meteorology  
UCLA  
Los Angeles, California 90024
31. LCDR P. G. Kesel, ODSI 1  
2460 Garden Road  
Monterey, California 93940
32. Mr. Leo C. Clarke 1  
Fleet Numerical Weather Central  
Naval Postgraduate School  
Monterey, California 93940
33. Naval Weather Service Command 1  
Washington Navy Yard  
Washington, D. C. 20390



34. Naval Oceanographic Office 1  
Library (Code 3330)  
Washington, D. C. 20373
35. Lieutenant William F. Mihok 5  
Fleet Numerical Weather Central  
Naval Postgraduate School  
Monterey, California 93940



REPORT DOCUMENTATION PAGE		READ INSTRUCTIONS BEFORE COMPLETING FORM
1. REPORT NUMBER	2. GOVT ACCESSION NO.	3. RECIPIENT'S CATALOG NUMBER
4. TITLE (and Subtitle) Global Weather Prediction Model Difference Schemes		5. TYPE OF REPORT & PERIOD COVERED Master's Thesis March 1974
		6. PERFORMING ORG. REPORT NUMBER
7. AUTHOR(s) William Franklin Mihok		8. CONTRACT OR GRANT NUMBER(s)
9. PERFORMING ORGANIZATION NAME AND ADDRESS Naval Postgraduate School Monterey, California 93940		10. PROGRAM ELEMENT, PROJECT, TASK AREA & WORK UNIT NUMBERS
11. CONTROLLING OFFICE NAME AND ADDRESS Naval Postgraduate School Monterey, California 93940		12. REPORT DATE March 1974
		13. NUMBER OF PAGES 58
14. MONITORING AGENCY NAME & ADDRESS (if different from Controlling Office) Naval Postgraduate School Monterey, California 93940		15. SECURITY CLASS. (of this report) Unclassified
		15a. DECLASSIFICATION/DOWNGRADING SCHEDULE
16. DISTRIBUTION STATEMENT (of this Report)  Approved for public release; distribution unlimited.		
17. DISTRIBUTION STATEMENT (of the abstract entered in Block 20, if different from Report)		
18. SUPPLEMENTARY NOTES		
19. KEY WORDS (Continue on reverse side if necessary and identify by block number)		
20. ABSTRACT (Continue on reverse side if necessary and identify by block number)  One case of analytic data and one case of real data were numerically integrated using a 5-level baroclinic primitive equation global model of the general circulation. The feasibility of using a mixed second order and fourth order space differencing scheme to improve the phase speeds of meteorological waves was examined. The results indicate that mixed scheme tends to give a better representation of the phase speeds than the second order scheme does.		





DD Form 1473 (BACK)  
1 Jan 73  
S/N 0102-014-6601







Thesis  
M5814 Mihok  
c.1

150553

Global weather predic-  
tion model difference  
schemes.

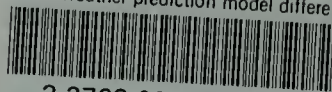
Thesis  
M5814 Mihok  
c.1

150553

Global weather predic-  
tion model difference  
schemes.

thesM5814

Global weather prediction model differen



3 2768 001 88327 5

DUDLEY KNOX LIBRARY